Proceedings of the 4th ITB Graduate School Conference
Innovation and Discovery for Sustainability
July 6, 2023

The Influence of Urea Mass on Photocatalytic Performance of N- TiO_2/CNC for CO_2 Reduction into Solar Fuel

Kapabihi[1], Haroki Madani[2], Arie Wibowo[4,5], Yogi Wibisono Budhi [2,3,5,*]

[1]Nanotechnology, Graduate School, Institut Teknologi Bandung, Jl. Ganesha 10, Bandung 40132, Indonesia.
[2]Departement of Chemical Engineering, Faculty of Industrial Technology, Institut Teknologi Bandung, Jalan Ganesha 10, Bandung 40132, Indonesia
[3]Research Group of Chemical Engineering Process Design and Development, Faculty of Industrial Technology, Institut Teknologi Bandung, Jalan Ganesha 10, Bandung 40132, Indonesia.
[4]Materials Science and Engineering Research Group, Faculty of Mechanical and Aerospace Engineering, Institut Teknologi Bandung, Jalan Ganesha 10, Bandung 40132, Indonesia.
[5]Research Center for Nanosciences and Nanotechnology, Institut Teknologi Bandung, Jalan Ganesha 10, Bandung 40132, Indonesia
*email: y.wibisono@itb.ac.id

Abstract. Photocatalysts are a promising method for converting CO2 with H2O into valuable products, such as hydrocarbon N-doped TiO2 catalysts synthesized in cellulose nanocrystals (CNC) using sol-gel. Then in this study, the mass of urea was varied (0, 0.0432, 0.864, and 0.1296 grams) to obtain N-doped TiO2/CNC samples, namely N0, N1, N2, and N3, respectively. The resulting N-doped TiO2/CNC and TiO2/CNC catalysts were characterized by TEM, Diffuse reflectance UV-Vis (DR UV-Vis) spectroscopy, and GC-XL analysis. TEM results showed evidence of particle sizes ranging from 26.7 nm for TiO2/CNC and 395.9 nm for CNC. The band gap energies obtained for N0, N1, N2, and N3 were 3.19, 3.18, 3.18, and 3.16 eV from DR UV-Vis spectroscopy, respectively. Then, in the activity test under visible light (λ = 380 nm), catalyst N2 exhibits superior photocatalyst activity than N0 for the reduction of CO2 with H2O because that nitrogen doping causes the formation of oxygen vacancies by generating intrinsic strain in the lattice of N0. However, catalysts N1 and N3 showed that no CH4 was detected. This study developed a photocatalyst using an N0 catalyst in visible light that effectively reduces CO2 with H2O.

Keywords: *CNC; Nitrogen; N0; Photocatalyst; Reduction CO_2.*

1 Introduction

Photocatalysts are a promising method for converting CO2 into valuable products, such as methane, hydrogen, methanol, formaldehyde, ethanol, and higher hydrocarbons [1]. TiO2 semiconductor is a widely studied photocatalyst due to its unique properties, high chemical stability, availability, and non-toxicity

[2]. However, TiO2 has a high electron-hole pair recombination rate and a band gap energy of 3.2 eV. Due to the wide band gap, the visible light activity of solar energy consists of about 4 - 5% UV light and 50% visible light [3]. Thus, in this study, it is necessary to develop a promising method to overcome the intrinsic limitations mentioned above, namely surface modification [4]. Surface modifications that can be used for TiO2 photocatalysts are ion doping [5], noble metal deposition [6], and heterojunction design [7]. TiO2 using ion doping has attracted widespread attention because it can increase photocatalyst activity. Then, TiO2 with N ion doping greatly supports the performance of photocatalysts because the increased activity of TiO2 photocatalyst in the visible light region provides good yield opportunities for wide applications such as oxidation of CO, ethanol, 2-propanol gas, acetaldehyde, and NOx and decomposition of dyes such as methylene blue [8].

In increasing the activity of TiO2 catalysts, using buffers in the synthesis of TiO2 photocatalysts can increase catalyst activity because it increases surface area; one of the buffers used is cellulose nanocrystals (CNC). CNC accelerates the nucleation and growth of TiO2 particles. Then, the hydroxyl groups of CNC help interact with TiO2 to increase the density of the formed nucleation, which will grow into nanocrystals through condensation reaction and promote the development of TiO2 particles [9]. In addition, CNC also prevents agglomeration and increases the surface area of TiO2 particles. CNC can be synthesized from various raw materials such as biomass [10], denim waste [11], oil palm [12-13], etc. [9] reported the synthesis of TiO2/CNC nanocomposite via in situ hydrolysis at 70 °C, which showed the presence of TiO2 particles on the surface of CNC. This study used CNC to synthesize N-doped TiO2/CNC catalyst using the sol-gel method, anatase TiO2 crystal, and a large specific surface area. The results show that the addition of N doping on TiO2/CNC catalyst can reduce the band gap.

2 Experimental methods

2.1 Materials

Titanium tetraisopropoxide (TTIP, 97.0%) was purchased from Sigma-Aldrich, Ethanol absolute (99.99%), nitric acid (69%), urea, and natrium hydroxide (50%) were purchased from Merck kGaA, Germany. Cellulose nanocrystal was purchased from Canada.

2.2 Synthesis of TiO2/CNC Catalyst

In a typical experiment, 1,2 ml of TTIP was mixed with 69 ml of ethanol absolute and stirred for 20 min. Nitric Acid 60 ml (65%) was added to the mixture under

vigorous stirring, and the solution was conditioned at room temperature. The solution's pH was controlled by adding 150 ml NaOH (1 M) to obtain sols at pH 4 and the addition of CNC as support. Then add nitrogen with various concentrations (0, 0.0432, 0.864, and 0.1296 grams) to obtain N-doped TiO2/CNC samples, namely N0, N1, N2, and N3. The sols were allowed to gel at room temperature (28 ℃) for 24 h. then centrifuged 3 times at 6000 rpm and finally dried.

2.3 Characterization

The synthesized TiO2/CNC samples were examined by High-resolution transmission electron microscopy (HRTEM, H9500, Japan) was used to study the particle size and distribution. Diffuse reflectance UV-Vis (DR UV-Vis) spectroscopy of the prepared samples was measured by a UV-Vis spectrophotometer (UV-2600, Shimadzu) with an integrating sphere attachment ranging from 200 to 800 nm, and TiO2 was used as a reflectance standard. The band gapenergy (Eg) for the direct band gap semiconductor was evaluated using the Kubelka-Munk.

2.4 Photocatalyst Reduction Test

Photocatalyst CO2 conversion experiments (Experiments in photocatalyst water reduction to produce chemical gas) were finished in a top-irradiation Pyrex flask. UV light (full wavelength 380 nm) became used as the light source. Typically, 8 mg photocatalysts had been dispersed in an 80 mL water solution under magnetic stirring. Before irradiation, CO2 gas will flow with a flow rate of 1 N/min for 6 hours. Whereas to evaluate the conversion of CO2 photocatalyst manufacturing, the fuel-phase composition of the photocatalyst reactor was analyzed every six hours by extracting 1 mL fluid and gas into gas chromatography GC-FID and GC-XL.

3 Results and Discussion

3.1 Morphology and crystal structure in TiO2/CNC photocatalyst

TEM images of the CNC and TiO2/CNC catalysts are shown in Figure 1. Figure 1a shows that the CNC appears as rod-like monocrystals with a diameter of 30,9 ± 18,9 nm and a length of 395,9 ± 207,2 nm. CNC dispersed in water has been used as a scaffold for TiO2 nanoparticles. Then in Figure 1b shows that TiO2/CNC has round and cubic shapes, while the particle size of TiO2 is 26,7 ± 15,6 nm in diameter.

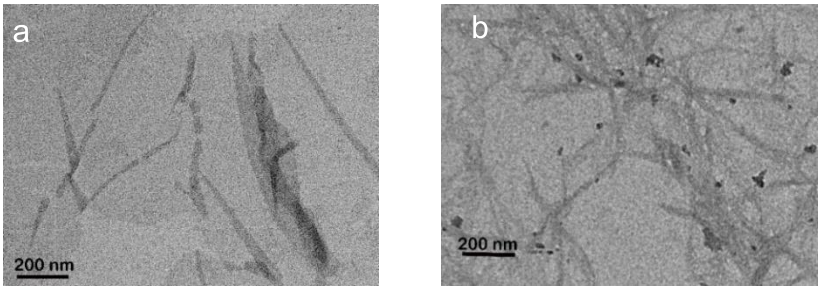

Figure 1 TEM images of a) CNC and b) CNC/TiO_2 Photocatalyst

Figure 1. There is a deposition reaction between CNC and TiO2 ions, TiO2 nanoparticles are dispersed above the surface of CNC (TiO2/CNC). This indicates that the presence of CNC can increase the density of nucleation formed, which will grow into nanocrystals and promote the development of TiO2 particles because the hydroxyl groups and sulfur groups of CNC help interact and limit the size of TiO2 [14]. This observation confirms the role of hydroxyl groups on CNC in increasing nucleation density during synthesis. In other words, the abundant hydroxyl groups can absorb Ti3+ ions and create nucleation sites on the surface of CNC [15].

3.2 The band gap in TiO2/CNC photocatalyst

The interaction between CNC and TiO2 can be investigated using UV-Vis spectra (Figure 2a), which shows a shift in the absorption spectrum for N-doped TiO2/CNC catalyst when compared to the undoped TiO2/CNC catalyst due to the narrowing of the band gap energy caused by the introduction of nitrogen atoms into the TiO2 lattice [16]. In addition, the UV absorption ability increases as the N-doped TiO2/CNC increases from N1 to N3. Then the Kubelka-Munk function can be used to estimate the band gap energy of these samples [17]. Since TiO2 is an indirect transition semiconductor, the band gap is obtained by using the plot of F(R)2 versus the absorbed light energy resulting in the band gaps of different

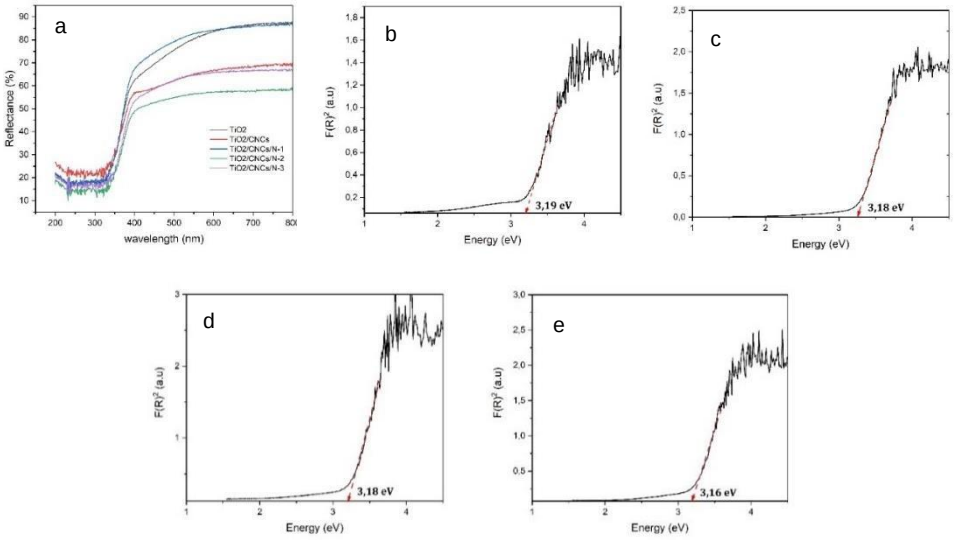

Figure 2 a) DR UV-Vis spectroscopy, band gap analysis, b) TiO_2, c) N0, d) N1, e) N2, f) N3.

3.3 TiO2 Photocatalyst activity test

This experiment controlled for the reduction of CO2 with H2O under UV irradiation at room temperature and a flow rate of 1 NL/min. In all experiments, continuous CH4, CO, and CH3OH production can be seen under UV irradiation, as shown in Figure 3a, with time variation using TiO2/CNC samples. It can be seen that the TiO2/CNC samples with a time of 2 hours and 4 hours did not detect the presence of CH4 and CH3OH. Because the reaction time of electrons coming out in the conduction band is insufficient, it takes time to collect electrons to reduce CO2 with H2O to CH4 and CH3OH. The conduction band (CB) of TiO2 is

0.50 eV at pH 7, the potential to reduce CO2 and H2O is -0.24 eV [20]. Since the conduction band potential is more favourable than the reduction potential of CO2 with H2O, this reaction is theoretically feasible. In addition, the production of CH4 and CO requires 8 electrons and 2 electrons, respectively [21]. The yield of CH4 production on the TiO2/CNC catalyst with a time of 6 hours is almost the same as that reported in the study [22] to reduce CO2 with H2O to CH4 via TiO2 catalyst with a value of 201 μmol/hour. At the same time, the CO yield decreased with time.

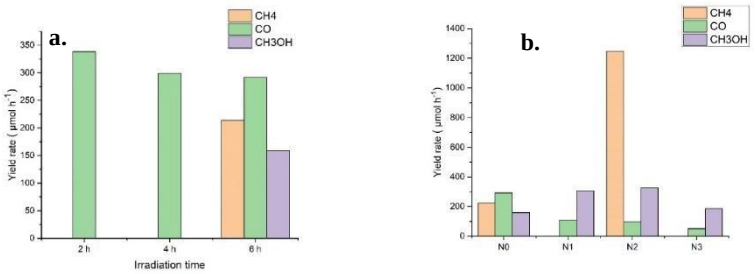

Figure 3 a) effect of irradiation time on CH4, CO, and CH3OH production with TiO2/CNC catalyst activity for CO2 photoreduction. b) effect of N doping addition on TiO2/CNC activity for CO2 reduction with H2O to CH4, CO and CH3OH during 6 hours of irradiation time

Figure 3b. Effect of adding N-doped into TiO2/CNC photocatalyst for CO2 reduction with H2O to CH4, CO, and CH3OH under UV light irradiation with a wavelength of 380 nm. The production of CO as the main product of CO2 reduction, lower CH4 was detected on the TiO2/CNC catalyst during 6 h of irradiation due to the rapid recombination of photon-generated electron-hole pairs

[23] and with the addition of nitrogen doping on the N2 catalyst can increase the CH4 product, indicating that nitrogen doping causes the formation of oxygen vacancies by generating intrinsic strain in the TiO2 lattice [24], which effectively inhibits recombination and improves the capture capacity of CO2 with H2O. However, the N1 and N3 catalysts showed no detectable CH4 due to the poor capture ability of CO2 with H2O and high recombination [25]. Thus the failure of electrons and protons to fulfill CH4 formation [26]. The N0 catalyst showed excellent activity for CO formation, but the addition of N-doped decreased CO production. CO production gradually decreases with increasing nitrogen doping [24].

4 Conclusion

The addition of nitrogen doping can reduce the bandgap value of TiO2, which is smaller because 2p nitrogen atoms can substitute with 2p O atoms. Thus narrowing the bandgap value of TiO2. Then the production of CH3OH and CH4 was detected on the N0 catalyst at 6 hours. This is electrons begin to collect and reduce CO2 with H2O. Then the production of CO decreased with the addition of time. Furthermore, the results of CH4 production with the addition of nitrogen doping showed that the N0 and N2 catalysts were detected, but the N1 and N3 catalysts were not detected. This was due to the lack of electrons, so the capture

and reduction of CO2 were poor. And for the results of CO decreased with the addition of nitrogen concentration.

Acknowledgment

The authors would like to acknowledge Institut Teknologi Bandung for providing financial support through Riset dan Inovasi ITB 2023.

References

[1] Sanchez, J.A, Carbon Dioxide Capture: Processes, Technology, and Environmental Implications; Nova Science Publishers (2016).
[2] Tahir, M., & Amin, N. S, Advances in visible light responsive titanium oxide-based photocatalysts for CO2 conversion to hydrocarbon fuels. Energy Conversion and Management, 76, 194-214 (2013).
[3] Ola, O., & Maroto-Valer, M. M, Review of material design and reactor engineering on TiO2 photocatalysis for CO2 reduction. Journal of Photochemistry and Photobiology C: Photochemistry Reviews, 24, 16-42 (2015).
[4] Low, J., Yu, J., Jaroniec, M., Wageh, S., & Al-Ghamdi, A. A, Heterojunction photocatalysts. Advanced materials, 29(20), 1601694.
[5] Kumar, S.G.K., dan Rao, Comparison of modification strategies towards enhanced charge carrier separation and photocatalytic degradation activity of metal oxide semiconductors (TiO2, WO3, and ZnO), Applied Surface Science, 391, 124–148 (2017).
[6] Lu, Q.L., Zhu, S., Han, Y., dan Hou, W. C, Photocatalytic Synthesis of Gold Nanoparticles Using TiO2 Nanorods: A Mechanistic Investigation, Physics Chemistry Chemistry Physics, 21, 18753–18757 (2019).
[7] He, F.A., Meng, B., Cheng, W, dan Ho, J.Y, Enhanced photocatalytic H2–production activity of WO3/TiO2 step–scheme heterojunction by graphene modification, Chin Journal Catalyst, 41, 9-20 (2020).
[8] Cong, Y. J., Zhang, F., Chen, dan Anpo, M, Synthesis and Characterization of Nitrogen-Doped TiO2 Nanophotocatalyst with High Visible Light Activity, Journal Physics Chemistry, 111, 6976-6982 (2007).
[9] Li, Y., Zhang, J., Zhan, C., Kong, F., Li, W., Yang, C., & Hsiao, B. S, Facile synthesis of TiO2/CNC nanocomposites for enhanced Cr (VI) photoreduction: Synergistic roles of cellulose nanocrystals. Carbohydrate polymers, 233, 115838 (2020).
[10] Restiawaty, E., Culsum, N. T. U., Nishiyama, N., & Budhi, Y. W., Preparation, characterization, and surface modification of cellulose nanocrystal from lignocellulosic biomass for immobilized lipase. Fibers, 10(4), 33, (2022).

[11] Culsum, N. T. U., Melinda, C., Leman, I., Wibowo, A., & Budhi, Y. W., Isolation and characterization of cellulose nanocrystals (CNCs) from industrial denim waste using ammonium persulfate. Materials Today Communications, 26, 101817 (2021).
[12] Wibowo, A. Madani, H. Judawisastra, Restiawaty, E. Lazarus, C. and Budhi, Y. W., An eco-friendly preparation of cellulose nanocrystals from oil palm empty fruit bunches. IOP conference series: earth and environmental science, 105, (2018).
[13] Budhi, Y. W., Fakhrudin, M., Culsum, N. T. U., Suendo, V., & Iskandar, F., Preparation of cellulose nanocrystals from empty fruit bunch of palm oil by using phosphotungstic acid. In IOP Conference Series: Earth and Environmental Science, 105(1), 012063, 2018.
[14] Virkutyte, J., Jegatheesan, V., & Varma, R. S, Visible light activated TiO2/microcrystalline cellulose nanocatalyst to destroy organic contaminants in water. Bioresource Technology, 113, 288-293 (2012).
[15] Li, Y., Zhang, J., Zhan, C., Kong, F., Li, W., Yang, C., & Hsiao, B. S, Facile synthesis of TiO2/CNC nanocomposites for enhanced Cr (VI) photoreduction: Synergistic roles of cellulose nanocrystals. Carbohydrate polymers, 233, 115838 (2020).
[16] Zhao, Y., Qiu, X., & Burda, C, The effects of sintering on the photocatalytic activity of N-doped TiO2 nanoparticles. Chemistry of Materials, 20(8), 2629-2636 (2008).
[17] Zhou, X., Lu, J., Jiang, J., Li, X., Lu, M., Yuan, G., ... & Seo, H. J, Simple fabrication of N-doped mesoporous TiO2 nanorods with the enhanced visible light photocatalytic activity. Nanoscale Research Letters, 9, 1-7 (2014).
[18] Marques, J., Gomes, T. D., Forte, M. A., Silva, R. F., & Tavares, C. J, A new route for the synthesis of highly active N-doped TiO2 nanoparticles for visible light photocatalysis using urea as nitrogen precursor. Catalysis Today, 326, 36-45 (2019).
[19] Wang, D. H., Jia, L., Wu, X. L., Lu, L. Q., & Xu, A. W, One-step hydrothermal synthesis of N-doped TiO2/C nanocomposites with high visible light photocatalytic activity. Nanoscale, 4(2), 576-584 (2012).
[20] Ong, C. B., Ng, L. Y., & Mohammad, A. W, A review of ZnO nanoparticles as solar photocatalysts: Synthesis, mechanisms, and applications. Renewable and Sustainable Energy Reviews, 81, 536-551 (2018).
[21] Tahir, B., Tahir, M., & Nawawi, M. G. M, highly stable 3D/2D WO3/g-C3N4 Z-scheme heterojunction for stimulating photocatalytic CO2 reduction by H2O/H2 to CO and CH4 under visible light. Journal of CO2 Utilization, 41, 101270 (2020).

[22] Tahir, M., & Amin, N. S, Indium-doped TiO2 nanoparticles for photocatalytic CO2 reduction with H2O vapors to CH4. Applied Catalysis B: Environmental, 162, 98-109 (2015).
[23] Tahir, M., & Tahir, B, Dynamic photocatalytic reduction of CO2 to CO in a honeycomb monolith reactor loaded with Cu and N doped TiO2 nanocatalysts. Applied Surface Science, 377, 244-252 (2016).
[24] Li, C., Sun, Z., Song, A., Dong, X., Zheng, S., & Dionysiou, D. D, Flowing nitrogen atmosphere induced rich oxygen vacancies overspread the surface of TiO2/kaolinite composite for enhanced photocatalytic activity within broad radiation spectrum. Applied Catalysis B: Environmental, 236, 76-87 (2018).
[25] Zhou, Y., Zhang, Q., Shi, X., Song, Q., Zhou, C., & Jiang, D, Photocatalytic reduction of CO2 into CH4 over Ru-doped TiO2: Synergy of Ru and oxygen vacancies. Journal of Colloid and Interface Science, 608, 2809-2819 (2022).
[26] Zhou, Y., Tian, Z., Zhao, Z., Liu, Q., Kou, J., Chen, X., ... & Zou, Z, High-yield synthesis of ultrathin and uniform Bi2WO6 square nanoplates benefiting from photocatalytic reduction of CO2 into renewable hydrocarbon fuel under visible light. ACS applied materials & interfaces, 3(9), 3594-3601 (2011).